# Importance of vector leptoquark-scalar box diagrams in Pati-Salam unification with vector-like families

Syuhei Iguro[1,2], Junichiro Kawamura[3], Shohei Okawa[4], and Yuji Omura[5]

[1]*Institute for Theoretical Particle Physics (TTP), Karlsruhe Institute of Technology (KIT), Engesserstraße 7, 76131 Karlsruhe, Germany*

[2]*Institute for Astroparticle Physics (IAP), Karlsruhe Institute of Technology (KIT), Hermann-von-Helmholtz-Platz 1, 76344 Eggenstein-Leopoldshafen, Germany*

[3]*Center for Theoretical Physics of the Universe, Institute for Basic Science (IBS), Daejeon 34051, Korea*

[4]*Departament de Física Quàntica i Astrofísica, Institut de Ciències del Cosmos (ICCUB), Universitat de Barcelona, Martí i Franquès 1, E-08028 Barcelona, Spain*

[5]*Department of Physics, Kindai University, Higashi-Osaka, Osaka 577-8502, Japan*

## Abstract

We study lepton flavor violating meson decays induced by box diagrams involving a vector leptoquark (LQ) and scalar fields in Pati-Salam (PS) unification with vector-like families. The vector LQ corresponds to the massive gauge boson associated with the PS gauge symmetry breaking and the scalar fields are the physical degrees of freedom of the PS breaking field. The LQ generally causes the rapid flavor violating decays, such as $K_L \to \mu e$, at the tree-level unless its mass scale is higher than PeV scale. The vector-like families are introduced to suppress the tree-level contributions mediated by the LQ and explain the realistic fermion mass matrices. In this paper, we point out that there are inevitable one-loop contributions to those meson decays from the box diagrams mediated by both one LQ and one scalar field, even if the tree-level contributions are suppressed. We consider a concrete model for demonstration, and find that the vector-like fermion masses have an upper bound for a given LQ mass when the one-loop induced meson decays are consistent with the experimental limits. The vector-like fermion mass should be lighter than 3 TeV for 20 TeV LQ, if a combination of the couplings does not suppress $K_L \to \mu e$ decay. Our findings would illustrate importance of the box diagrams involving both LQ and physical modes of symmetry breaking scalars in generic models.

KEYWORDS: Pati-Salam, Vector leptoquark, Box diagrams, Lepton flavor violation

# Contents

# 1 Introduction

The Pati-Salam (PS) unification [1] is a compelling new physics scenario, given an ambitious motivation as a potential pathway toward grand unified theories. In recent years, with growing interests in empirical hints for new physics found in flavor violating observables, significant attention has been paid to PS models and variants thereof with TeV scale symmetry breaking. Indeed, a vector leptoquark (LQ), appearing as a result of the PS symmetry breaking, has the same quantum number as a well-studied single mediator solution to the $R_{K^{(*)}}$ [2–10] and $R_{D^{(*)}}$ [11–20] anomalies. Furthermore, such a particle could also account for the muon $g-2$ anomaly [21–25].

In the basic construction of the PS unification, lowering the PS symmetry breaking scale faces two difficulties. First, PS models partly unify quarks and leptons and hence predict the common mass matrices to them, that obviously contradicts the observed fermion spectra. Secondly, the vector LQ associated with the symmetry breaking carries both baryon and lepton numbers and couples quarks and leptons flavor-dependently at the tree-level. These couplings easily induce various lepton flavor violating meson decays that are almost forbidden in the Standard Model (SM) [26]. In the conventional setup, the $K_L \to \mu e$ decay brings the most severe limit and pushes the PS breaking scale to be heavier than 1 PeV [27, 28].

In recent studies, mainly stimulated by the $B$ meson anomalies, it has been shown that both problems can be resolved by introducing vector-like fermions mixed with the SM chiral fermions [29–31]. In this way, imposing relations between PS conserving vector-like masses and those originated from PS breaking, the vector LQ does not couple to a SM lepton and quark simultaneously and thus the leptonic neutral meson decays are absent at the tree-level. This solution, however, relies on a 0.1% level tuning between the PS conserving and breaking masses to have the TeV-scale vector LQ without conflicting with the strong flavor constraints [31]. Since any symmetry does not forbid the flavor violations through the LQ in this scenario and the constraint from the $K_L \to \mu e$ decay requires much higher PS breaking scale based on the naive dimensional analysis, even loop induced effects may exclude the TeV-scale LQ in the PS models with vector-like fermions.

Loop effects on flavor violations in new physics models with LQs have been discussed in connection with the $B$ anomalies based on a PS model [29], 4321 models [32, 33] and composite model [34]. In these works, the $b \to c$ transition turns out to correlate with the $B_s$ mixing induced by box diagrams with two LQs or two scalars. It has been found that the $R_{D^{(*)}}$ anomaly can be explained consistently when the Glashow-Iliopoulos-Maiani (GIM) like mechanism [35] works for those box diagrams.

In this paper, we study another class of box diagrams which involve one vector LQ and one scalar, and evaluate the impact of such diagrams on the leptonic neutral meson decays. As a demonstration, we consider a simple PS model only with vector-like copies of the SM chiral fermions and an $SU(4)_C$ adjoint scalar field in addition to the three generations of chiral fermions.[1]. We especially focus on flavor violating processes among down-type quarks and charged leptons. In this setup, we compute all box diagrams relevant to the rare meson decays of our interest. As

---

[1]Additional scalar fields are necessary to break the residual $SU(2)_R \times U(1)_{B-L}$ gauge symmetry as well as the see-saw mechanism for the neutrino masses. We do not discuss its explicit realization since this would not affect the flavor violations discussed in this work.

Table 1: The matter content in the Pati-Salam model.

| fields | spin | $SU(4)_C$ | $SU(2)_L$ | $SU(2)_R$ |
|:------:|:----:|:---------:|:---------:|:---------:|
| $L$ | 1/2 | **4** | **2** | **1** |
| $F_L$ | 1/2 | **4** | **2** | **1** |
| $F_R$ | 1/2 | **4** | **2** | **1** |
| $R$ | 1/2 | **4** | **1** | **2** |
| $f_R$ | 1/2 | **4** | **1** | **2** |
| $f_L$ | 1/2 | **4** | **1** | **2** |
| $\Delta$ | 0 | **15** | **1** | **1** |
| $\Phi$ | 0 | **1** | **2** | **$\overline{2}$** |

a result, we shall identify the specific coupling structures in the Wilson coefficients of the semi-leptonic operators. We find that some coefficients are cancelled because of the GIM-like mechanism due to the unitarity of the LQ couplings, while such cancellation is absent in the coefficients induced by the box diagrams involving both LQ and adjoint scalar. The latter coefficients are, thus, not suppressed by the GIM-like mechanism and induce the rapid lepton flavor violating meson decays. We also observe that these unsuppressed pieces are proportional to the power of the ratio of the vector-like fermion mass to the LQ mass. This indicates that upper limits on the vector-like fermion masses are obtained for a given LQ mass when the limit from the rare meson decays is respected. Interestingly, the vector-like fermions reside below the TeV scale if the PS symmetry breaking scale is TeV-scale as favored by the anomalies of the $B$-meson decays.

This paper is organized as follows. In Sec. 2, we construct our PS model and explain how the observed mass spectra are realized by introducing vector-like fermions in addition to chiral ones. We also explain the reason that the box diagrams involving both the LQ and the scalars induce the leptonic neutral meson decays. In Sec. 3, the box-diagram contributions to the semi-leptonic operators are evaluated and the non-vanishing coupling structures are identified. We perform numerical analysis of the one-loop contributions in Sec. 4 and discuss the impact on the PS model construction. Section 5 is devoted to summary.

## 2 Pati-Salam model with TeV-scale vector LQ

### 2.1 Schematic picture to suppress tree-level flavor violation

We consider a model with the PS gauge symmetry, $SU(4)_C \times SU(2)_L \times SU(2)_R$. The PS symmetry identifies the lepton number as a fourth color of the $SU(4)_C$, and SM chiral quark and lepton fields with the same $SU(2)_L$ representation are unified in chiral fields, $L_i$ and $R_i$ ($i = 1, 2, 3$), whose representations are respectively $(\mathbf{4}, \mathbf{2}, \mathbf{1})$ and $(\mathbf{4}, \mathbf{1}, \mathbf{2})$ under the PS symmetry. The electroweak (EW) doublet Higgs field is embedded in a bi-doublet field of $SU(2)_L \times SU(2)_R$, namely $\Phi$ whose

representation is $(\mathbf{1}, \mathbf{2}, \overline{\mathbf{2}})$, leading to two EW doublet Higgs fields at the low energy. With this minimal content, general Yukawa interaction is given by

$$-\mathcal{L}_Y^{\min} = \overline{L}Y_1\Phi R + \overline{L}Y_2\epsilon^T\Phi^*\epsilon R + h.c., \tag{2.1}$$

where $\epsilon := i\sigma_2$ acts onto the $SU(2)_L$ and $SU(2)_R$ indices and $Y_1$ and $Y_2$ are $3\times3$ Yukawa matrices in the flavor space. A massive vector LQ, $X^\mu$, appears as a result of the $SU(4)_C \to SU(3)_C \times U(1)_{B-L}$ breaking. The gauge interaction is

$$\mathcal{L}_X = \frac{g_4}{\sqrt{2}}X_\mu\left(\overline{d}_L^i\gamma^\mu e_L^i + \overline{u}_L^i\gamma^\mu\nu_L^i + \overline{d}_R^i\gamma^\mu e_R^i + \overline{u}_R^i\gamma^\mu\nu_R^i\right) + h.c.. \tag{2.2}$$

Note that the gauge interaction is flavor diagonal and universal unless the $SU(4)_C$ breaking effects to the fermion masses are taken into account. The interaction terms in Eqs. (2.1) and (2.2) explicitly show two problems inherent in the minimal construction of the PS model. One is that the minimal Yukawa terms Eq. (2.1) predict the same mass matrices for quarks and leptons, i.e. $m_e^{ij} = m_d^{ij}$ and $m_u^{ij} = m_\nu^{ij}$. The other is that the LQ interaction Eq. (2.2) mediates $\overline{d}_id_j \to \overline{e}_ie_j$ processes at the tree-level and triggers the rapid $K_L \to \mu e$ decay.

These problems are resolved by introducing $SU(4)_C$ charged scalar fields and vector-like fermions in addition to $L^i$ and $R^i$. Before proceeding to the general argument, we briefly demonstrate our basic idea to create the mass splitting with a particular focus on the down-type quarks and charged leptons. The up-type quark and neutrino masses can be achieved independently of the discussion below. For the demonstrative purpose, we only focus on a single generation of $L^i$ and add one vector-like copy $F_{L,R} = (\mathbf{4}, \mathbf{2}, \mathbf{1})$ and an $SU(4)_C$ adjoint scalar field $\Delta$ [29,31]. With this extended content, we can write down additional interaction terms,

$$-\mathcal{L}_M = \overline{L}(m_L + \kappa_L\Delta)F_R + \overline{F}_L(M_L + Y_L\Delta)F_R + h.c., \tag{2.3}$$

where $m_L$ and $M_L$ are the PS symmetric mass parameters. Decomposing the fermions

$$L = \begin{pmatrix} \nu_L & e_L \\ u_L & d_L \end{pmatrix}, \quad F_A = \begin{pmatrix} N_A & E_A \\ U_A & D_A \end{pmatrix}, \tag{2.4}$$

with $A = L, R$ and after the adjoint field develops the vacuum expectation value (VEV) $\langle\Delta\rangle = v_\Delta/(2\sqrt{3})\mathrm{diag}(3, -1, -1, -1)$, the mass terms split as

$$-\mathcal{L}_M = \overline{d_L}\left(m_L - \frac{\kappa_Lv_\Delta}{2\sqrt{3}}\right)D_R + \overline{D_L}\left(M_L - \frac{Y_Lv_\Delta}{2\sqrt{3}}\right)D_R$$
$$+ \overline{e_L}\left(m_L + \frac{3\kappa_Lv_\Delta}{2\sqrt{3}}\right)E_L + \overline{E_L}\left(M_L + \frac{3Y_Lv_\Delta}{2\sqrt{3}}\right)E_R + \cdots, \tag{2.5}$$

where we only show the down-type quarks and charged leptons. Imposing the cancellation conditions,

$$m_L - \frac{\kappa_Lv_\Delta}{2\sqrt{3}} = 0, \quad M_L + \frac{3Y_Lv_\Delta}{2\sqrt{3}} = 0, \tag{2.6}$$

only $(D_L, D_R)$ and $(e_L, E_R)$ have vector-like masses,

$$-\mathcal{L}_M = \left( M_L - \frac{Y_L v_\Delta}{2\sqrt{3}} \right) \overline{D_L} D_R + \left( m_L + \frac{3\kappa_L v_\Delta}{2\sqrt{3}} \right) \overline{e_L} E_R + \cdots , \qquad (2.7)$$

whereas $d_L$ and $E_L$ remain massless which are identified as the SM fermions. These massless quark and lepton respectively originate in the different PS multiplets, $L$ and $F_L$. This indicates that unlike the minimal model, they have different Yukawa couplings to the bi-doublet scalar $\Phi$, which in turn results in different mass matrices for the quark and lepton. The left-handed LQ couplings are now in the form of

$$\mathcal{L}_X = \frac{g_4}{\sqrt{2}} X_\mu (\overline{d_L} \gamma^\mu e_L + \overline{D_L} \gamma^\mu E_L) + \cdots . \qquad (2.8)$$

Since $e_L$ and $D_L$ are heavy, the LQ coupling always involves heavy fermions, not mediating the leptonic meson decays at the tree level. It should be noted that the EW gauge interactions remain unchanged under this exchanging of the $SU(2)_L$ doublets $e_L$ and $E_L$. The mass splitting of the right-handed quark and lepton is realized by introducing a corresponding vector-like copy in an analogous way.

Now we have seen the generation of the mass splitting by introducing the vector-like fermions. Following this method and adding more vector-like families, we can realize the observed mass spectra and the suppressed neutral meson decays in the three generation case [31]. On the other hand, this trick predicts a specific interaction structure that will revive the meson decays via one-loop box diagrams. To see this, we explicitly keep the radial mode of $\Delta$ by the replacement $v_\Delta \to v_\Delta + h_\Delta$ in Eq. (2.5). We then obtain Yukawa interactions of $h_\Delta$,

$$-\mathcal{L}_M = -\frac{\kappa_L}{2\sqrt{3}} h_\Delta \overline{d_L} D_R + \frac{3Y_L}{2\sqrt{3}} h_\Delta \overline{E_L} E_R + \cdots . \qquad (2.9)$$

Although there is no mass term in the form of $\overline{d_L} D_R$ and $\overline{E_L} E_R$, the couplings of $h_\Delta \overline{d_L} D_R$ and $h_\Delta \overline{E_L} E_R$ are present. Thus, the $d \to e$ transition comes back via the interaction to the radial mode $h_\Delta$,

$$\frac{g_4 \kappa_L}{2\sqrt{6} M_D} h_\Delta X_\mu \overline{d_L} \gamma^\mu E_L, \qquad (2.10)$$

where we assume that the vector-like fermions are heavy and integrate them out (see also Fig. 1). We note that $E_L$ is a SM-like lepton. Further integrating out the LQ and $h_\Delta$, we will obtain semi-leptonic operators that contribute to the leptonic neutral meson decays such as $K_L \to \mu e$.

One may wonder if other box diagrams involving two LQs or two $h_\Delta$ scalars can also induce the same semileptonic operators. This is true indeed, but as we will show in the rest of this paper, such contributions enjoy the GIM-like suppression and can be negligibly small. On the contrary, the LQ-scalar box contributions via the combination of Eqs. (2.8) and (2.9) have no such suppression and thus are unavoidable. The evaluation of the LQ-scalar box diagrams is the main aim of this paper. In the following, we will study a realistic version of the PS extension highlighted above and perform analytical and numerical analyses to derive quantitative limits on the model.
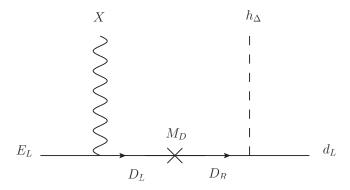
Figure 1: A schematic picture of regenerating the $d \to e$ transition via the interaction to the radial mode of the PS symmetry breaking scalar $h_\Delta$.

## 2.2 Realistic model

In this section, we generalize the discussion above to accommodate the realistic quark and lepton masses. We introduce $N_L$ vector-like $SU(2)_L$ doublet fermions $F_{L,R}$ and $N_R$ vector-like $SU(2)_L$ singlet fermions $f_{L,R}$ in addition to $L^i$, $R^i$ and $\Phi$. $F_L$ and $f_R$ are assumed to possess the same quantum numbers as that of $L$ and $R$, respectively, and $F_R$ and $f_L$ are their vector-like pairs. The relevant part of Lagrangian is given by

$$-\mathcal{L}_M = \overline{F}_L \left(M_L + Y_L \Delta\right) F_R + \overline{L}\left(m_L + \kappa_L \Delta\right) F_R + \overline{f}_L \left(M_R + Y_R \Delta\right) f_R + \overline{f}_L \left(m_R + \kappa_R \Delta\right) R + \cdots,$$
(2.11)

where all couplings and masses are considered as matrices in the flavor space and the ellipsis represents interactions between the fermions and the Higgs bi-doublet field $\Phi$. The fermions are decomposed to quarks and leptons as

$$L = \begin{pmatrix} \nu_L & e_L \\ u_L & d_L \end{pmatrix}, \quad R = \begin{pmatrix} \nu_R & e_R \\ u_R & d_R \end{pmatrix}, \quad F_A = \begin{pmatrix} N_A & E_A \\ U_A & D_A \end{pmatrix}, \quad f_A = \begin{pmatrix} \mathcal{N}_A & \mathcal{E}_A \\ \mathcal{U}_A & \mathcal{D}_A \end{pmatrix},$$
(2.12)

where the index $A = L, R$. The scalar fields obtain non-vanishing VEVs,

$$\langle \Delta \rangle = \frac{v_\Delta}{2\sqrt{3}} \begin{pmatrix} 3 & 0 \\ 0 & -\mathbf{1}_3 \end{pmatrix}, \quad \langle \Phi \rangle = v_H \begin{pmatrix} \cos\beta & 0 \\ 0 & \sin\beta \end{pmatrix}.$$
(2.13)

The matter contents of the model is summarized in Table 1.

## 2.3 Mass matrix

We shall see the mass mixing of the fermions, which is directly linked to the coupling structure of the LQ and scalars. We mainly discuss flavor violating processes among the down-type quarks

and charged leptons in this paper, so that we only show the terms relevant to them.[2] Without loss of generality, the fermion mass terms are given by

$$-\mathcal{L}_{\text{mass}} = \overline{\mathbf{d}}_L \mathcal{M}_d \mathbf{d}_R + \overline{\mathbf{e}}_L \mathcal{M}_e \mathbf{e}_R \tag{2.14}$$

$$:= \begin{pmatrix} \overline{d}_L \\ \overline{D}_L \\ \overline{\mathcal{D}}_L \end{pmatrix}^T \begin{pmatrix} m_{33} & m_{3R} & 0_{3\times N_L} \\ m_{L3} & m_{LR} & D_{d_L} \\ 0_{N_R \times 3} & D_{d_R} & m_{RL} \end{pmatrix} \begin{pmatrix} d_R \\ \mathcal{D}_R \\ D_R \end{pmatrix} + \begin{pmatrix} \overline{e}_L \\ \overline{E}_L \\ \overline{\mathcal{E}}_L \end{pmatrix}^T \begin{pmatrix} m_{33} & m_{3R} & M_{eE} \\ m_{L3} & m_{LR} & M_{EE} \\ M_{\mathcal{E}e} & M_{\mathcal{E}\mathcal{E}} & m_{RL} \end{pmatrix} \begin{pmatrix} e_R \\ \mathcal{E}_R \\ E_R \end{pmatrix}$$

where $D_{d_A}$ is an $N_A \times N_A$ diagonal matrix with $A = L, R$ and $m_{\alpha\beta}$ ($\alpha, \beta = 3, L, R$) is an $N_\alpha \times N_\beta$ mass matrix of $\mathcal{O}(v_H)$. Here, $N_\alpha = 3$ for $\alpha = 3$. Note that the structure of $m_{\alpha\beta}$ is common to $\mathcal{M}_d$ and $\mathcal{M}_e$ due to the PS symmetry. We define the mass basis for the fermions:

$$\hat{\mathbf{d}}_A = U_{d_A}^\dagger \mathbf{d}_A, \quad \hat{\mathbf{e}}_A = U_{e_A}^\dagger \mathbf{e}_A. \tag{2.15}$$

The unitary matrices, $U_{f_A}$ ($f = e, d$), diagonalize the mass matrices as

$$U_{f_L}^\dagger \mathcal{M}_f U_{f_R} = \text{diag}\left(m_1^f, m_2^f, m_3^f, \cdots, m_{N_L+N_R+3}^f\right). \tag{2.16}$$

The three lightest fermions correspond to the SM fermions and there are $N_L + N_R$ extra fermions.

We are interested in the approximate forms of the unitary matrices when $\eta := m_{\alpha\beta}/v_\Delta \ll 1$ [3], and only keep the leading contribution by neglecting $\mathcal{O}(\eta)$ effects. Assuming the elements of $D_{d_L}$ and $D_{d_R}$ are larger than the other elements, the masses of the chiral three families ($d_L$, $d_R$) are expected to be given by $m_{33}$ dominantly. We note that the elements of $m_{33}$ are $\mathcal{O}(v_H)$. Then, ($d_L$, $d_R$) does not mix with the vector-like families at the leading order in $\eta$, and these down-type quarks are SM-like. The charged leptons ($e_L, e_R$) do not, on the other hand, correspond to the SM families due to the vector-like masses $M_{\mathcal{E}e}$ and $M_{eE}$. The vector-like masses for the charged leptons can be, in general, decomposed as

$$\begin{pmatrix} M_{eE} \\ M_{EE} \end{pmatrix} =: V_L \begin{pmatrix} D_{e_L} \\ 0_{3\times N_L} \end{pmatrix} W_R^\dagger, \quad \left(M_{\mathcal{E}e} \; M_{\mathcal{E}\mathcal{E}}\right) =: W_L \left(0_{N_R\times 3} \; D_{e_R}\right) V_R^\dagger, \tag{2.17}$$

where $V_A$ and $W_A$ are $(3+N_A) \times (3+N_A)$ and $N_{\overline{A}} \times N_{\overline{A}}$ unitary matrices, respectively, where $\overline{A}$ denotes the opposite chirality of $A$, i.e. $\overline{A} = R, L$ for $A = L, R$. $D_{e_A}$ is a diagonal $N_A \times N_A$ matrix with real positive entries. Hence, the unitary matrices are approximately given by

$$U_{d_L} = \begin{pmatrix} \mathbf{1}_3 & 0 & 0 \\ 0 & 0 & \mathbf{1}_{N_L} \\ 0 & \mathbf{1}_{N_R} & 0 \end{pmatrix}, \quad U_{d_R} = \begin{pmatrix} \mathbf{1}_3 & 0 & 0 \\ 0 & \mathbf{1}_{N_R} & 0 \\ 0 & 0 & \mathbf{1}_{N_L} \end{pmatrix}, \tag{2.18}$$

$$U_{e_L} = \begin{pmatrix} V_L & 0_{(3+N_L)\times N_R} \\ 0_{N_R\times(3+N_L)} & W_L \end{pmatrix} P, \quad U_{e_R} = \begin{pmatrix} 0_{(3+N_R)\times N_L} & V_R \\ W_R & 0_{N_L\times(3+N_R)} \end{pmatrix} P,$$

---

[2]See Ref. [31] for the full detail of the mass mixing and diagonalization including the up-type quarks and neutrinos.

[3]If the $\mathcal{O}(v_H)$ entries are at most the bottom quark mass, we find $\eta \lesssim 10^{-3}$ for $v_\Delta \sim 4$ TeV.

with

$$P := \begin{pmatrix} 0 & 0 & \mathbf{1}_{N_L} \\ \mathbf{1}_3 & 0 & 0 \\ 0 & \mathbf{1}_{N_R} & 0 \end{pmatrix}. \tag{2.19}$$

Here, the matrix $V_L$ ($V_R$) represents the mixing within the $SU(2)_L$ doublets (singlets) in the left-handed (right-handed) sectors, while the matrix $W_L$ ($W_R$) is the mixing within the $SU(2)_L$ singlets (doublets) in the left-handed (right-handed) sector. The vanishing blocks of $U_{e_A}P^{-1}$ reflect the fact that the $SU(2)_L$ doublet and singlet do not mix each other without the VEV of $\Phi$. These blocks have non-vanishing entries of $\mathcal{O}(\eta)$ or smaller in fact. With the unitary matrices $U_{d_A}$ and $U_{e_A}$ in this form, the mass matrices are approximately diagonalized as

$$U_{d_L}^\dagger \mathcal{M}_d U_{d_R} = \begin{pmatrix} m_{33} & m_{3R} & 0 \\ 0 & D_{d_R} & m_{RL} \\ m_{L3} & m_{LR} & D_{d_L} \end{pmatrix} =: D_d, \quad U_{e_L}^\dagger \mathcal{M}_e U_{e_R} = \begin{pmatrix} \widetilde{m}_{33} & \widetilde{m}_{3R} & 0 \\ 0 & D_{e_R} & \widetilde{m}_{RL} \\ \widetilde{m}_{L3} & \widetilde{m}_{LR} & D_{e_L} \end{pmatrix} =: D_e, \tag{2.20}$$

where

$$V_L^\dagger \begin{pmatrix} m_{33} & m_{3R} \\ m_{L3} & m_{LR} \end{pmatrix} V_R =: \begin{pmatrix} \widetilde{m}_{L3} & \widetilde{m}_{LR} \\ \widetilde{m}_{33} & \widetilde{m}_{3R} \end{pmatrix}, \quad W_L^\dagger m_{RL} W_R =: \widetilde{m}_{RL}. \tag{2.21}$$

Neglecting the sub-dominant effects suppressed by $\eta$, the mass matrices of the SM down-type quarks and charged leptons are determined by $m_{33}$ and $\widetilde{m}_{33}$, respectively. Their singular values should be consistent with the SM fermion masses up to $\mathcal{O}(\eta)$ corrections. The other elements of $m_{\alpha\beta}$ and $\widetilde{m}_{\alpha\beta}$ give only sub-dominant effects to the mixing matrices as far as the vector-like fermions are sufficiently heavier than the EW scale.

## 2.4 Couplings with the vector LQ and scalars in $\Delta$

The $SU(4)_C$ gauge symmetry is broken by the VEV of the adjoint scalar $\Delta$. The massive gauge boson $X_\mu$ associated with the $SU(4)_C \to SU(3)_c \times U(1)_{B-L}$ breaking arises as a vector LQ. If $\Delta$ only breaks the $SU(4)_C$ symmetry, the LQ mass $m_X$ is given by

$$m_X = \frac{2}{\sqrt{3}} g_4 v_\Delta, \tag{2.22}$$

where $g_4$ denotes the $SU(4)_C$ gauge coupling. This relation is modified if further scalars contribute to the $SU(4)_C$ breaking.

The gauge couplings to the fermions are given by

$$\mathcal{L}_X = \frac{g_4}{\sqrt{2}} X^\mu \left( \overline{\mathbf{d}}_L \gamma_\mu \mathbf{e}_L + \overline{\mathbf{d}}_R \gamma_\mu \mathbf{e}_R \right) + h.c. \tag{2.23}$$

$$= X^\mu \left( \overline{\widehat{\mathbf{d}}}_L \hat{g}_L \gamma_\mu \hat{\mathbf{e}}_L + \overline{\widehat{\mathbf{d}}}_R \hat{g}_R \gamma_\mu \hat{\mathbf{e}}_R \right) + h.c..$$

The LQ couplings in the mass basis are expressed by

$$\hat{g}_L = \frac{g_4}{\sqrt{2}}\Omega_L, \quad \hat{g}_R = \frac{g_4}{\sqrt{2}}\Omega_R, \quad \text{with} \quad \Omega_L := U^\dagger_{d_L}U_{e_L}, \quad \Omega_R := U^\dagger_{d_R}U_{e_R}. \tag{2.24}$$

Defining

$$V_L =: \begin{pmatrix} V_{3L} & X_L \\ Y_L & V_{L3} \end{pmatrix}, \quad V_R =: \begin{pmatrix} X_R & V_{3R} \\ V_{R3} & Y_R \end{pmatrix}, \tag{2.25}$$

$\Omega_{L,R}$ are approximately given by

$$\Omega_L = \begin{pmatrix} X_L & 0 & V_{3L} \\ 0 & W_L & 0 \\ V_{L3} & 0 & Y_L \end{pmatrix}, \quad \Omega_R = \begin{pmatrix} X_R & V_{3R} & 0 \\ V_{R3} & Y_R & 0 \\ 0 & 0 & W_R \end{pmatrix}. \tag{2.26}$$

It should be noted that the $3 \times 3$ matrix $X_A$ in $V_A$ represents overlapping of the SM charged leptons $\hat{e}^i_A$ with the first three PS multiplets $L^i$ and $R^i$ which the SM down-type quarks $\hat{d}^i_A$ mostly originate in. Thus, we see in Eq. (2.26) that $X_A$ stands for the LQ couplings to two SM fermions. As a reminder, taking $X_A = 0$ corresponds to the cancellation in Eq. (2.6).

After the $SU(4)_C$ breaking, the adjoint scalar $\Delta$ is decomposed into a singlet scalar $h_\Delta$ and an $SU(3)_c$ adjoint scalar $\Delta_8$:

$$\Delta = \frac{1}{2\sqrt{3}}\left(v_\Delta + \frac{h_\Delta}{\sqrt{2}}\right)\begin{pmatrix} 3 & 0 \\ 0 & -\mathbf{1}_3 \end{pmatrix} + \begin{pmatrix} 0 & 0 \\ 0 & \Delta_8 \end{pmatrix}, \tag{2.27}$$

where $\mathbf{1}_n$ denotes an $n \times n$ identity matrix. The Yukawa couplings involving $h_\Delta$ and $\Delta_8$ are given by

$$-\mathcal{L}_\Delta = \sum_{\mathbf{f}=\mathbf{d},\mathbf{e}} \sqrt{\frac{3}{8}} h_\Delta Q^{\mathbf{f}}_{B-L} \bar{\mathbf{f}}_L Y_\Delta \mathbf{f}_R + \Delta_8 \bar{\mathbf{d}}_L Y_\Delta \mathbf{d}_R + h.c., \tag{2.28}$$

where $Q^{\mathbf{d}}_{B-L} = -1/3$ and $Q^{\mathbf{e}}_{B-L} = +1$ are the $B-L$ charges. In the mass basis, the couplings are given by

$$\hat{Y}^f_\Delta = \left(U^f_L\right)^\dagger Y_\Delta U^f_R, \quad f = d, e. \tag{2.29}$$

Since the interaction to $\Delta$ generates the mass splitting of the down-type quarks and charged leptons, there is a close relation between the Yukawa coupling matrices in the gauge basis and the fermion mass matrices,

$$Y_\Delta = \frac{\sqrt{3}}{2v_\Delta}\left(\mathcal{M}_e - \mathcal{M}_d\right). \tag{2.30}$$

9

Using this relation, the Yukawa matrices in the mass basis are expressed as

$$\hat{Y}_\Delta^e = \frac{\sqrt{3}}{2v_\Delta}\left(D_e - \Omega_L^\dagger D_d \Omega_R\right) + \mathcal{O}\left(\eta\right). \quad \hat{Y}_\Delta^d = \frac{\sqrt{3}}{2v_\Delta}\left(\Omega_L D_e \Omega_R^\dagger - D_d\right) + \mathcal{O}\left(\eta\right). \quad (2.31)$$

It follows that the flavor violating couplings are induced via

$$\Omega_L^\dagger D_d \Omega_R \sim \begin{pmatrix} 0 & 0 & V_{L3}^\dagger D_{d_L} W_R \\ W_L^\dagger D_{d_R} V_{R3} & W_L^\dagger D_{d_R} Y_R & 0 \\ 0 & 0 & Y_L^\dagger D_{d_L} W_R \end{pmatrix} + \mathcal{O}\left(m_{\alpha\beta}\right), \quad (2.32)$$

$$\Omega_L D_e \Omega_R^\dagger \sim \begin{pmatrix} 0 & 0 & V_{3L} D_{e_L} W_R^\dagger \\ W_L D_{e_R} V_{3R}^\dagger & W_L D_{e_R} Y_R^\dagger & 0 \\ 0 & 0 & Y_L D_{e_L} W_R^\dagger \end{pmatrix} + \mathcal{O}\left(m_{\alpha\beta}\right). \quad (2.33)$$

The tree-level couplings of $h_\Delta$ and $\Delta_8$ to the SM families are suppressed by $\eta$.

# 3 Flavor violations from box diagrams

In this section, we look at box contributions to flavor violating processes, using the LQ and scalar couplings to the fermions derived in the previous section.

## 3.1 Tree-level constraints

We first summarize the constraints set by considering only the tree-level LQ exchange, which motivate us to impose a primary suppression condition. It follows from Eq. (2.26) that the LQ couplings to the SM fermions are given by $X_L$ and $X_R$. With these couplings, the tree LQ exchange induces the semi-leptonic operators in the form of

$$\mathcal{L}_{\text{eff}} = \frac{g_4^2}{2m_X^2} \sum_{A,B=L,R} (X_A)^{ik}(X_B^\dagger)^{lj}(\overline{d}_A^i \gamma^\mu e_A^k)(\overline{e}_B^l \gamma_\mu d_B^j), \quad (3.1)$$

leading to various leptonic meson decays, e.g. $K_L \to \mu e$, $B_d \to \tau e$, $B_s \to \tau\mu$ and so on. We show in Appendix B rough estimates of experimental bounds on $X_L$ and $X_R$, assuming $m_X = 5\,\text{TeV}$ and $g_4 = 1$. This set of bounds suggests that if all elements of $X_A$ have comparable size, each matrix element should satisfy

$$\left|(X_L)^{ij}\right|, \left|(X_R)^{ij}\right| \lesssim \mathcal{O}(10^{-3}). \quad (3.2)$$

This limit motivates us to set a condition for suppressed flavor violation:
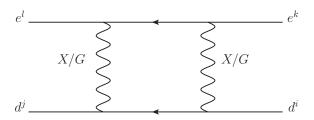
(i) $X_L = X_R = 0$ .

Figure 2: The box diagram involving LQ and Goldstone boson.

Given this condition, the unitarity of $V_A$ requires that $N_A \geq 3$ and

$$V_{3A}V_{3A}^\dagger \simeq V_{A3}^\dagger V_{A3} \simeq \mathbf{1}_3. \tag{3.3}$$

It is noted that the exchange of $h_\Delta$ and $\Delta_8$ does not cause flavor violation at the tree-level, since the Yukawa couplings of $h_\Delta$ and $\Delta_8$ always contain heavy fermions as seen in Eqs. (2.31), (2.32) and (2.33). Therefore, once the condition (i) is imposed, the model is free from the flavor violation at the tree-level.

## 3.2   Box contributions

We shall look at box-diagram contributions to semi-leptonic operators. Let us start with the box diagrams involving two LQs shown in Fig. 2. Under the condition (i), the LQ couplings with two SM fermions are vanishing (i.e. $X_A = 0$), so that we can only consider the vector-like fermions in the loop. In the diagram where the internal fermion mass is not picked up, the external fermions maintain the chirality. Such contribution is given in the form of

$$(g_4)^4 \sum_{I,J \geq 4} f(m_I^e, m_J^d; m_X, m_X) \big[\Omega_A^\dagger\big]_{lI}\big[\Omega_A\big]_{Ik}\big[\Omega_B\big]_{jJ}\big[\Omega_B^\dagger\big]_{Ji}, \tag{3.4}$$

where $A, B = L, R$ and $I, J = 4, 5, \cdots, N_L + N_R + 3$ run only over the vector-like fermions. Given the unitarity of the LQ couplings $\Omega_A$, this equation reminds us of the well-known GIM mechanism. Hence, we now suggest another suppression condition,

(ii)  vector-like fermion masses are universal: $m_I^d =: m_D$ and $m_I^e =: m_E$ for $I \geq 4$ .

This condition corresponds to $D_{d_L} \simeq m_D \mathbf{1}_{N_L}$, $D_{d_R} \simeq m_D \mathbf{1}_{N_R}$, $D_{e_L} \simeq m_E \mathbf{1}_{N_L}$ and $D_{e_R} \simeq m_E \mathbf{1}_{N_R}$ up to $\mathcal{O}(\eta)$ contributions. In case the conditions (ii) is satisfied as well as the condition (i), the loop function $f(m_I^e, m_J^d; m_X, m_X)$ can be pulled out of the summation over the internal fermion species and then we recognize the GIM-like suppression:

$$\sum_{I \geq 4}\big[\Omega_A^\dagger\big]_{lI}\big[\Omega_A\big]_{Ik} \sim \big[V_{L3}^\dagger V_{L3}\big]_{lk} \sim \delta_{lk}, \tag{3.5}$$
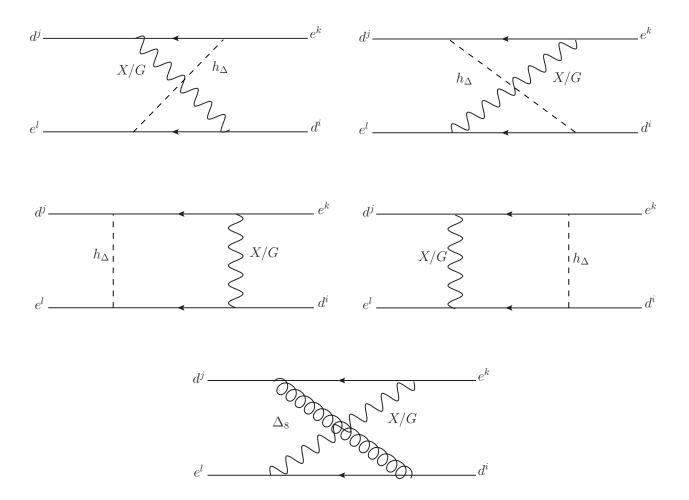
Figure 3: The box diagrams involving scalars and LQ/Goldstone.

where Eq. (3.3) is used. We can also show that the unitarity assures a similar suppression in the other combination $[\Omega_B]_{jJ}[\Omega_B^\dagger]_{Ji} \sim \delta_{ji}$ where the summation over vector-like species $J$ is taken. Flavor violating processes with $i \neq j$ or $k \neq l$ are therefore suppressed by the unitarity of $\Omega_A$.

When the internal fermion mass is picked up, the chirality of the external fermions is flipped and different coupling combinations, e.g. $\Omega_L^\dagger D_d \Omega_R$, appear in the Wilson coefficients. Such contribution contains the factor,

$$m_D \sum_{I \geq 4} [\Omega_A^\dagger]_{lI} [\Omega_{\overline{A}}]_{Ik} \sim 0, \tag{3.6}$$

where the condition (ii) is assumed. This result reflects the fact that there is no mixing between $SU(2)_L$ singlet and doublet fermions. Thus, any sizable flavor violation is not induced via the box diagram involving two LQs once the conditions (i) and (ii) are imposed.
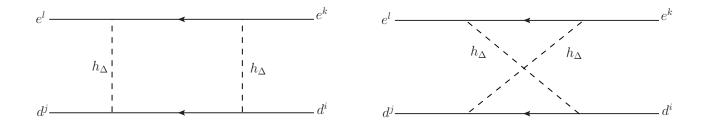
Figure 4: The box diagrams involving only scalars.

We next examine the box diagrams with $h_\Delta$ or $\Delta_8$ in the loop. There are two categories of diagrams: box diagrams involving one LQ and one scalar shown Fig. 3 and diagrams involving only scalars shown Fig. 4. These diagrams generate the semi-leptonic operators,

$$
\begin{aligned}
i\mathcal{L}_{\text{eff}} &= C_{VLL}^{ij,kl} \left( \overline{d}_L^j \gamma_\mu d_L^i \right) \left( \overline{e}_L^l \gamma_\mu e_L^k \right) + C_{VRR}^{ij,kl} \left( \overline{d}_R^j \gamma_\mu d_R^i \right) \left( \overline{e}_R^l \gamma_\mu e_R^k \right) \\
&+ C_{VRL}^{ij,kl} \left( \overline{d}_R^j \gamma_\mu d_R^i \right) \left( \overline{e}_L^l \gamma_\mu e_L^k \right) + C_{VLR}^{ij,kl} \left( \overline{d}_L^j \gamma_\mu d_L^i \right) \left( \overline{e}_R^l \gamma_\mu e_R^k \right) \\
&+ C_{SLL}^{ij,kl} \left( \overline{d}_R^j d_L^i \right) \left( \overline{e}_R^l e_L^k \right) + C_{SRR}^{ij,kl} \left( \overline{d}_L^j d_R^i \right) \left( \overline{e}_L^l e_R^k \right) \\
&+ C_{SRL}^{ij,kl} \left( \overline{d}_L^j d_R^i \right) \left( \overline{e}_R^l e_L^k \right) + C_{SLR}^{ij,kl} \left( \overline{d}_R^j d_L^i \right) \left( \overline{e}_L^l e_R^k \right),
\end{aligned}
\tag{3.7}
$$

where the flavors of the quarks and leptons are different ($i \neq j$ and $k \neq l$), in which the experimental constraints are the most stringent. Under the conditions (i) and (ii) and assuming $m_{h_\Delta} = m_{\Delta_8}$ for simplicity, the Wilson coefficients are given by

$$
C_{VAA}^{ij,kl} = \frac{3m_E^2 m_D^2}{8v_\Delta^4 m_X^2} \Upsilon_A^{li} \Upsilon_A^{*\,kj} \left[ \frac{3}{16} G_1(m_E, m_D; m_X, m_{h_\Delta}) - \frac{g_4^2 v_\Delta^2}{m_X^2} G_0(m_E, m_D; m_X, m_{h_\Delta}) \right], \tag{3.8}
$$

$$
C_{VA\overline{A}}^{ij,kl} = 0, \tag{3.9}
$$

$$
C_{SAA}^{ij,kl} = \frac{9m_E^3 m_D^3}{512 v_\Delta^4 m_X^4} \Psi_A^{lk} \overline{\Psi}_A^{ji} \widetilde{F}_0(m_E, m_D; m_{h_\Delta}, m_{h_\Delta}), \tag{3.10}
$$

$$
C_{SA\overline{A}}^{ij,kl} = \frac{3m_E^2 m_D^2}{4v_\Delta^4 m_X^2} \Upsilon_A^{li} \Upsilon_A^{*\,kj} \left[ -\frac{3}{16} G_1(m_E, m_D; m_X, m_{h_\Delta}) + \frac{g_4^2 v_\Delta^2}{m_X^2} G_0(m_E, m_D; m_X, m_{h_\Delta}) \right] \tag{3.11}
$$

$$
+ \frac{m_E^3 m_D^3}{8v_\Delta^4 m_X^4} \Psi_A^{lk} \overline{\Psi}_A^{*\,ji} \widetilde{F}_0(m_E, m_D; m_{h_\Delta}, m_{h_\Delta}),
$$

where the loop functions $\widetilde{F}_0, G_0$ and $G_1$ are defined in App. A. The diagrams with one LQ and one scalar contribute to $C_{VAA}$ and $C_{SA\overline{A}}$, while the diagrams with two $h_\Delta$ contributes to $C_{SAA}$ and $C_{SA\overline{A}}$. Note that the box diagram involving one LQ and one Goldstone boson is vanishing.

Those box contributions are expressed in terms of the combinations of the unitary matrices,

$$
\Upsilon_A := \Omega_A^\dagger P_{\overline{3}} \Omega_{\overline{A}} P_{\overline{3}} \Omega_A^\dagger, \quad \Psi_A := \Omega_A^\dagger P_{\overline{3}} \Omega_{\overline{A}} P_{\overline{3}} \Omega_A^\dagger P_{\overline{3}} \Omega_A, \quad \overline{\Psi}_A := \Omega_A P_{\overline{3}} \Omega_{\overline{A}}^\dagger P_{\overline{3}} \Omega_A P_{\overline{3}} \Omega_A^\dagger, \tag{3.12}
$$

13

where $P_{\bar{3}} := \mathrm{diag}\,(0,0,0,1,\cdots,1)$ is a projection matrix to the vector-like families. $\Psi$ and $\overline{\Psi}$ are originated from the diagrams only with the scalars. Using Eq. (2.26), the explicit structures are given by

$$
\Psi_L = \begin{pmatrix} 0 & 0 & V_{L3}^\dagger W_R Y_L^\dagger W_R \\ W_L^\dagger Y_R W_L^\dagger V_{R3} & W_L^\dagger Y_R W_L^\dagger Y_R & 0 \\ 0 & 0 & Y_L^\dagger W_R Y_L^\dagger W_R \end{pmatrix}, \tag{3.13}
$$

$$
\Psi_R = \begin{pmatrix} 0 & V_{R3}^\dagger W_L Y_R^\dagger W_L & 0 \\ 0 & Y_R^\dagger W_L Y_R^\dagger W_L & 0 \\ W_R^\dagger Y_L W_R^\dagger V_{L3} & 0 & W_R^\dagger Y_L W_R^\dagger Y_L \end{pmatrix}, \tag{3.14}
$$

$$
\overline{\Psi}_L = \begin{pmatrix} 0 & 0 & V_{3L} W_R^\dagger Y_L W_R^\dagger \\ W_L Y_R^\dagger W_L V_{3R}^\dagger & W_L Y_R^\dagger W_L Y_R^\dagger & 0 \\ 0 & 0 & Y_L W_R^\dagger Y_L W_R^\dagger \end{pmatrix}, \tag{3.15}
$$

$$
\overline{\Psi}_R = \begin{pmatrix} 0 & V_{3R} W_L^\dagger Y_R W_L^\dagger & 0 \\ 0 & Y_R W_L^\dagger Y_R W_L^\dagger & 0 \\ W_R Y_L^\dagger W_R V_{3L}^\dagger & 0 & W_R Y_L^\dagger W_R Y_L^\dagger \end{pmatrix}. \tag{3.16}
$$

Since the top-left $3 \times 3$ blocks are zero, flavor violations via these coupling structures are expected to be suppressed under the conditions (i) and (ii). The situation is different in the diagrams involving both LQ and adjoint scalars. The contributions are proportional to $\Upsilon_L$ or $\Upsilon_R$ which are given by

$$
\Upsilon_L = \begin{pmatrix} V_{L3}^\dagger W_R V_{3L}^\dagger & 0 & V_{L3}^\dagger W_R Y_L^\dagger \\ 0 & W_L^\dagger Y_R W_L^\dagger & 0 \\ Y_L^\dagger W_R V_{3L}^\dagger & 0 & Y_L^\dagger W_R Y_L^\dagger \end{pmatrix}, \quad \Upsilon_R = \begin{pmatrix} V_{R3}^\dagger W_L V_{3R}^\dagger & V_{R3}^\dagger W_L Y_R^\dagger & 0 \\ Y_R^\dagger W_L V_{3R}^\dagger & Y_R^\dagger W_L Y_R^\dagger & 0 \\ 0 & 0 & W_R^\dagger Y_L W_R^\dagger \end{pmatrix}. \tag{3.17}
$$

We find that the SM top-left blocks are $3 \times 3$ unitary matrices and cannot be vanishing. Note that one of the two indices of $\Upsilon_{L,R}^{li}$ represents quark flavor and the other represents lepton flavor. Thus, even if the SM blocks in $\Upsilon_{L,R}^{li}$ are diagonal, it does not indicate that flavor violating processes with $i \neq j$ and $k \neq l$ are vanishing. Indeed, we will see in the next section that when we take $\Upsilon_{L,R}^{li} = \delta_{li}$, the rapid $K_L \to \mu e$ decay is caused.

The above results can be understood as follows. Without the $SU(2)_L$ breaking effects, the Yukawa couplings of $\Delta$ with the SM leptons $e_{L,R}$ are schematically given by

$$
\Delta \left( \bar{e}_L Y_{e_L} E_R + \overline{\mathcal{E}}_L Y_{e_R} e_R \right) + h.c., \tag{3.18}
$$

where $E_R$ $(\mathcal{E}_L)$ is the $SU(2)_L$ doublet (singlet) heavy lepton. Hence, the SM leptons with different chirality cannot participate in the same Yukawa couplings of $\Delta$ without the $SU(2)_L$ breaking effects. As a result, non-zero box contributions with two scalars are proportional to $Y_{e_L}^\dagger Y_{e_L}$ or

Table 2: Values of masses $m_M$, lifetimes $\tau_M$ and decay constants $f_M$ of the mesons $M = K, B_d, B_s$ [36, 37].

| $M$ | $m_M$ [GeV] | $\tau_M$ [$\times 10^{12} \cdot$ GeV$^{-1}$] | $f_M$ [GeV] |
|---|---|---|---|
| $K$ | 0.4976 | $7.773 \times 10^4$ | 0.1552 |
| $B_d$ | 5.280 | 2.308 | 0.1920 |
| $B_s$ | 5.367 | 2.320 | 0.2284 |

$Y_{e_R}^\dagger Y_{e_R}$ which are diagonal under the condition (ii). Thus, no flavor violating interaction is induced via those diagrams. On the other hand, once the LQ interactions of the SM down quarks $d_{L,R}$

$$X^\mu \left( g_{d_L} \overline{d}_L \gamma_\mu E_L + g_{d_R} \overline{d}_R \gamma_\mu \mathcal{E}_R \right) + h.c., \tag{3.19}$$

are considered, the SM down-type quarks can interact with the SM charged leptons via the vector-like leptons. Such contribution has the coupling structure of $Y_{e_R} g_{d_R}$ or $Y_{e_L}^\dagger g_{d_L}$, which corresponds to $\Upsilon_{L,R}$ and hence is non-vanishing. $\Upsilon_{L,R}$ is also understood as a generalized version of $g_4 \kappa_L$ in Eq. (2.10).

As a side remark, we comment on the flavor violation in four-quark and four-lepton operators. Based on our finding in this section, the unsuppressed coupling structure $\Upsilon_{L,R}$ is obtained only from the box diagrams with one LQ and one $h_\Delta$ (or $\Delta_8$). Such diagrams only show up in the $\overline{d}_i d_j \to \overline{e_k} e_l$ processes and do not induce the four-quark and four-lepton operators. The latter operators are only generated from the box diagrams with two LQs or two $h_\Delta$, providing the coupling structures of $\Omega_A \Omega_A^\dagger$, $\Omega_A \Omega_{\overline{A}}^\dagger$, $\Psi$, or $\overline{\Psi}$ that only contain flavor-conserving or vanishing elements for the SM fermions. Therefore, the flavor violations originated from four-quark and four-lepton operators are suppressed under the conditions (i) and (ii).

# 4 Phenomenology

We evaluate the lepton flavor violating meson decays, assuming the condition (i) and (ii). We see that there is an upper limit on the vector-like fermion mass for a given LQ mass when experimental bounds from those decays are respected.

## 4.1 Flavor violating leptonic decays of neutral mesons

Rare meson decays $M_{ij} \to e_k^- e_l^+$, where $M_{ij}$ is a meson composed of $\overline{d}_j d_i$, are the key processes induced from the semi-leptonic operators of our interest. In general, the partial decay width of $M_{ij} \to e_k^- e_l^+$ is given by

$$\Gamma(M_{ij} \to e_k^- e_l^+) = \frac{f_M^2 \beta}{16\pi m_M} \left[ \left( m_M^2 - m_l^2 - m_k^2 \right) a^{ij,kl} - b^{ij,kl} \right], \tag{4.1}$$

$$a^{ij,kl} = \sum_{A=L,R} \left| \overline{m}_M S_A^{ij,kl} - m_l V_A^{ij,kl} + m_k V_{\overline{A}}^{ij,kl} \right|^2, \tag{4.2}$$

$$b^{ij,kl} = 4 m_k m_l \mathrm{Re} \left[ \left( \overline{m}_M S_L^{ij,kl} - m_l V_L^{ij,kl} + m_k V_R^{ij,kl} \right) \left( \overline{m}_M S_R^{ij,kl} - m_l V_R^{ij,kl} + m_k V_L^{ij,kl} \right)^* \right], \tag{4.3}$$

$$V_A^{ij,kl} := \frac{C_{VRA}^{ij,kl} - C_{VLA}^{ij,kl}}{2}, \quad S_A^{ij,kl} := \frac{C_{SRA}^{ij,kl} - C_{SLA}^{ij,kl}}{2}, \tag{4.4}$$

where $f_M$ and $m_M$ is a decay constant and mass of a meson $M$, and

$$\beta := \sqrt{1 - 2\frac{m_l^2 + m_k^2}{m_M^2} + \frac{(m_l^2 - m_k^2)^2}{m_M^4}}. \tag{4.5}$$

Here, we used

$$\langle 0|\overline{d}_j \gamma^\mu \gamma_5 d_i | M_{ij} \rangle = i f_M P_M^\mu, \quad \langle 0|\overline{d}_j \gamma_5 d_i | M_{ij} \rangle = -i f_M \overline{m}_M, \tag{4.6}$$

where $P_M^\mu$ is a four momentum of a meson $M$ and $\overline{m}_M := m_M^2/(m_{d_i} + m_{d_j})$ with $m_{d_i}$ being mass of quark $d_i$. Since the mass scales of the meson and LQ are hierarchically different, the RG corrections of the strong coupling constant are included by replacing in Eq. (4.6), [30]

$$\overline{m}_M \to \overline{m}_M R_M(m_X), \tag{4.7}$$

where

$$R_M(m_X) := R(m_M, m_c; 3) R(m_c, m_b; 4) R(m_b, m_t; 5) R(m_t, m_X; 6), \tag{4.8}$$

with

$$R(\mu_1, \mu_2; n_f) := \left( \frac{g_3(\mu_1)}{g_3(\mu_2)} \right)^{\frac{8}{11 - 2n_f/3}}. \tag{4.9}$$

Here we assume that all the new particles are $\mathcal{O}(m_X)$ and much higher than the top quark mass. Values of the meson parameters used in our calculation are shown in Table 2. Hence, the branching fractions are given by

$$\mathrm{BR}(M_{ij} \to e_k e_l) \simeq \tau_M \left\{ \Gamma(M_{ij} \to e_k^- e_l^+) + \Gamma\left(M_{ij} \to e_k^+ e_l^-\right) \right\}. \tag{4.10}$$

The experimental upper bounds on the branching fractions are shown in Table 3.

## 4.2 Simplified analysis

We shall compare the box-induced meson decays with the experimental limits. For concreteness, we consider $N_L = N_R = 3$ that is the minimal option to realize $X_L = X_R = 0$. We neglect the sub-dominant effects suppressed by $\eta$, and thus the flavor violation is induced only via $\Upsilon_{L,R}^{ij}$ which

Table 3: Decay modes of neutral mesons. The leptonic indices $(k, l)$ are added with its counterpart $(l, k)$.

| observable | upper limit | $(i, j)$, $(k, l)$ | | Ref. |
|---|---|---|---|---|
| BR $(K_L \to \mu e)$ | $4.7 \times 10^{-12}$ | $(1, 2)$, | $(1, 2)$ | [36] |
| BR $(B_d \to \mu e)$ | $1.0 \times 10^{-9}$ | $(1, 3)$, | $(1, 2)$ | [36] |
| BR $(B_d \to \tau e)$ | $2.8 \times 10^{-5}$ | $(1, 3)$, | $(1, 3)$ | [36] |
| BR $(B_d \to \tau \mu)$ | $1.4 \times 10^{-5}$ | $(1, 3)$, | $(2, 3)$ | [36] |
| BR $(B_s \to \mu e)$ | $5.4 \times 10^{-9}$ | $(2, 3)$, | $(1, 2)$ | [36] |
| BR $(B_s \to \tau e)$ | - | $(2, 3)$, | $(1, 3)$ | [36] |
| BR $(B_s \to \tau \mu)$ | $4.2 \times 10^{-5}$ | $(2, 3)$, | $(2, 3)$ | [36] |

corresponds to the SM blocks of $\Upsilon_{L,R}$. In this case, $\Upsilon_{L,R}^{ij}$ are $3 \times 3$ unitary matrices and are treated as input parameters in our study. We further assume that the SM down-type fermions are in the mass basis for a given $\Upsilon_{L,R}^{ij}$, i.e.

$$m_{33} \simeq \text{diag}\,(m_d, m_s, m_b)\,, \quad \widetilde{m}_{33} \simeq V_{L3}^\dagger m_{LR} V_{R3} \simeq \text{diag}\,(m_e, m_\mu, m_\tau)\,. \tag{4.11}$$

We impose the relations to the mass parameters

$$m_{\text{VL}} := m_E = m_D\,, \quad m_{h_\Delta} = m_X \tag{4.12}$$

and Eq. (2.22) for the LQ mass with $g_4 = 1$ to be consistent with the strong coupling constant at the TeV scale. Input parameters in our analysis are

$$m_X, \quad m_{\text{VL}}, \quad \Upsilon_L^{ij}, \quad \Upsilon_R^{ij}. \tag{4.13}$$

Among the decays, $K_L \to \mu e$ is the most sensitive to new physics contribution. The branching fraction is given by

$$\text{BR}\,(K_L \to \mu e) \simeq \frac{\tau_K m_K f_K^2}{16\pi m_X^4} |C_0|^2 \left(1 - \frac{m_\mu^2}{m_K^2}\right)^2 \sum_{A=L,R} \sum_{p=1,2} \left|\Upsilon_A^{2p}\right|^2 \left|\overline{m}_K \Upsilon_{\overline{A}}^{1\overline{p}} - \frac{m_\mu}{2}\Upsilon_A^{1\overline{p}}\right|^2, \tag{4.14}$$

where $\overline{p} = 2, 1$ for $p = 1, 2$, and

$$C_0 := \frac{9m_{\text{VL}}^4}{16v_\Delta^4}\left(\frac{1}{4}G_1(m_{\text{VL}}, m_{\text{VL}}; m_X, m_X) - G_0(m_{\text{VL}}, m_{\text{VL}}; m_X, m_X)\right) \tag{4.15}$$

are defined and the electron mass is neglected. With the sizable chiral enhancement proportional to $\overline{m}_K$, we find the branching fraction to be

$$\text{BR}\,(K_L \to \mu e) \simeq 3.5 \times 10^{-5} \times \left|\Upsilon_A^{2p}\Upsilon_{\overline{A}}^{1\overline{p}}\right|^2 \left(\frac{|C_0|}{16\pi^2}\right)^2 \left(\frac{5\text{ TeV}}{m_X}\right)^4, \tag{4.16}$$
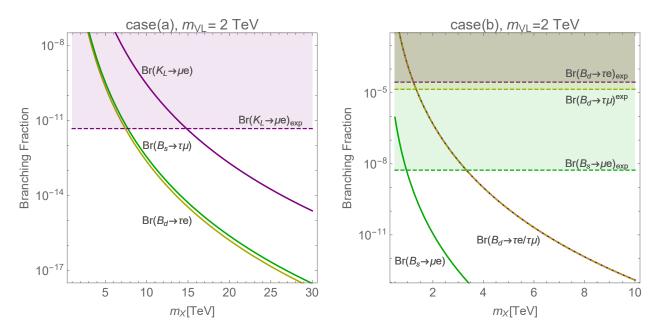
Figure 5: Values of the branching fractions in the simplified scenarios with $m_{\mathrm{VL}} = 2$ TeV. $\mathrm{BR}\,(B_d \to \tau e) \simeq \mathrm{BR}\,(B_d \to \tau \mu)$ in the case (b).

while without the chiral enhancement,

$$\mathrm{BR}\,(K_L \to \mu e) \simeq 3.0 \times 10^{-9} \times \left|\Upsilon_A^{2p} \Upsilon_A^{1\bar{p}}\right|^2 \left(\frac{|C_0|}{16\pi^2}\right)^2 \left(\frac{5\ \mathrm{TeV}}{m_X}\right)^4. \tag{4.17}$$

Hence there should be $\mathcal{O}\,(10^{-7})$ and $\mathcal{O}\,(10^{-3})$ suppression from the couplings and masses with and without the chiral enhancement. It is illuminating to give the scaling of the loop function $C_0$ with $m_{\mathrm{VL}} \ll m_X$,

$$|C_0| \simeq \frac{m_{\mathrm{VL}}^4}{8\pi^2 m_X^4} \left(\frac{7}{4} + \log \frac{m_{\mathrm{VL}}^2}{m_X^2}\right). \tag{4.18}$$

In this limit, the branching fraction is proportional to $(m_{\mathrm{VL}}/m_X)^8$. The mass splitting of the LQ and the vector-like fermions will help to suppress the branching fraction.

We consider the two simplified cases:

$$\text{(a)}\quad \Upsilon_L^{ij} = \Upsilon_R^{ij} = \delta_{ij} \quad \text{and} \quad \text{(b)}\quad \Upsilon_L^{ij} = \begin{pmatrix} 0 & 1 & 0 \\ 0 & 0 & 1 \\ 1 & 0 & 0 \end{pmatrix}, \ \Upsilon_R^{ij} = \begin{pmatrix} 0 & 0 & 1 \\ 0 & 1 & 0 \\ 1 & 0 & 0 \end{pmatrix}. \tag{4.19}$$

In the case (a), there is a large contribution to $K_L \to \mu e$ via $\Upsilon_A^{11} \Upsilon_A^{22}$. Whereas, in the case (b), there is no contribution to $K_L \to \mu e$ and $B_d \to \mu e$ and further the chiral enhanced contributions to $B_s \to \mu e$ are vanishing. Hence, the analyses in the cases (a) and (b) result in the strongest and weakest limits, respectively.
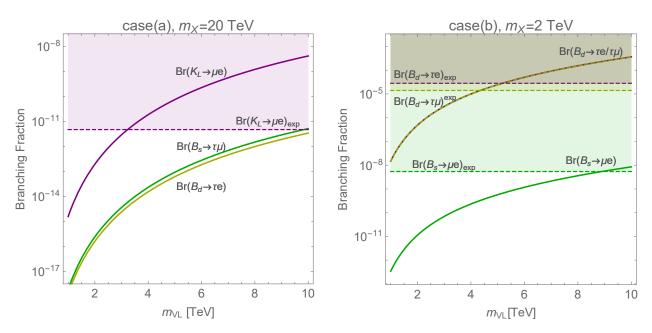
Figure 6: Values of the branching fractions in the simplified scenarios with $m_X = 20$ (2) TeV in the left (right) panel. $\mathrm{BR}\,(B_d \to \tau e) \simeq \mathrm{BR}\,(B_d \to \tau\mu)$ in the case (b).

Figures 5 and 6 show values of the branching fractions in the cases (a) and (b). The solid lines are our predictions in this model and the horizontal dashed lines are the experimental limits. Note that the other decay modes not shown in the figures are vanishing in the simplified scenarios. In the case (a), the LQ mass should be heavier than 15 TeV for $m_{\mathrm{VL}} = 2$ TeV and there is an upper bound on $m_{\mathrm{VL}} \lesssim 3$ TeV when $m_X = 20$ TeV from $\mathrm{BR}\,(K_L \to \mu e)$, whereas $\mathrm{BR}\,(B_d \to \tau\mu)$ and $\mathrm{BR}\,(B_s \to \tau e)$ are much smaller than the experimental limits of $\mathcal{O}\,(10^{-5})$. It is remarkable that the branching fraction is suppressed via $m_{\mathrm{VL}}^4/v_\Delta^4$ in $C_0$, providing an *upper* bound on the vector-like masses for a given LQ mass. In the case (b), the limits are weaker because of the vanishing contribution to $\mathrm{BR}\,(K_L \to \mu e)$, and hence $m_X = 2$ TeV is heavy enough to be consistent with the limits. Among the decay modes, $\mathrm{BR}\,(B_d \to \tau\mu)$ provides the most stringent limit of 4 TeV. The limits from $\mathrm{BR}\,(B_s \to \mu e)$ is weaker in spite of the severe experimental limits, since the chiral enhancement contribution is absent in this case.

Let us comment on the LHC constraints on the model. In our analysis, we consider the vector-like fermions heavier than 2 TeV that are significantly higher than the current LHC limits around 1 TeV [38, 39]. Thus we need higher energy colliders, e.g. $\sqrt{s} = 100$ TeV to explore the allowed parameter space shown in Fig 6. There is also the strong constraint of 5 TeV on $Z'$ from the di-muon resonance search [40]. Hence the light LQ scenarios would be excluded if a scalar field which violates $U(1)_{B-L}$ gives a large contribution to the LQ mass. In fact, 2 TeV LQ is not allowed when the $U(1)_{B-L}$ is broken by a scalar field with $(\overline{10}, 1, 3)$ under the PS symmetry [31]. Thus, the LQ lighter than a few TeV may be excluded by the $Z'$ boson search depending on the model.
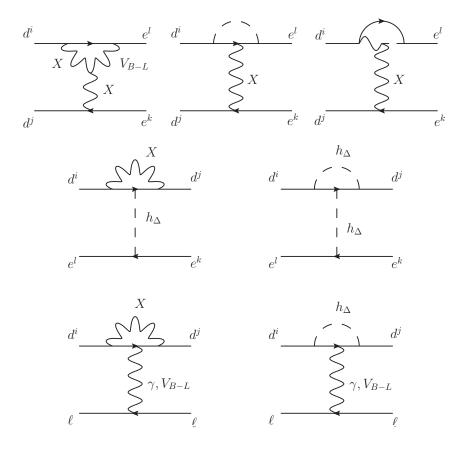
Figure 7: Example one-loop penguin contributions to semi-leptonic operators, $(\overline{d}_j \Gamma d_i)(\overline{e}_k \Gamma e_l)$ and $(\overline{d}_j \Gamma d_i)(\overline{\ell} \Gamma \ell)$.

## 4.3 Comments on penguin diagrams

We comment on contributions from one-loop penguin diagrams, which may generate flavor violation comparable with the box contributions.[4] Figure 7 shows examples of the contributing diagrams. They fall into two categories; one violates both quark and lepton flavor and another violates either of them but not both. Diagrams in the first and second lines of Fig. 7 belong to the first category and can generate quark and lepton flavor violating operators in the form $(\overline{d}_j \Gamma d_i)(\overline{e_k} \Gamma e_l)$ where $\Gamma$ represents an arbitrary Lorentz structure. As discussed above, such operators lead to the $K_L \to \mu e$ decay and thus to the severe constraint. These contributions, however, contain a tree-level coupling, namely $\Omega_{L,R}^{jk}$, $(\hat{Y}_\Delta^e)^{kl}$ or $(\hat{Y}_\Delta^d)^{ji}$, and are always suppressed under the condition (i).

In the second category, lepton flavor conserving processes $\overline{d_j} d_i \to \ell\bar{\ell}$ are induced via photon and $V_{B-L}$ penguin diagrams (the third line of Fig. 7) even though we require the condition (i).

---

[4]There are two-loop contributions: two sets of one-loop vertex corrections involving a LQ and an adjoint scalar. However, such contributions are suppressed by the loop factor, couplings and the power of $m_{\rm VL}^2/m_X^2$ and thus expected to be smaller than the one-loop box contribution.

Here, let us have a closer look at the coupling structure of such contributions. In the diagrams with the LQ loop, the amplitudes of such processes contain the following structures

$$\sum_I (\Omega_{L,R})^{jI}(\Omega_{L,R}^\dagger)^{Ii} \; f(m_I^e, m_X), \quad \sum_I (\Omega_L)^{jI}(\Omega_R^\dagger)^{Ii} \; g(m_I^e, m_X), \qquad (4.20)$$

where $f$ and $g$ are loop functions. Now they depend on the LQ couplings to the vector-like families. Assuming the condition (ii), the former contribution is vanishing for $i \neq j$ because of the unitarity of the LQ couplings $\Omega_{L,R}$, Eq. (3.3). The latter contribution is proportional to $(\Omega_L)^{jI}(\Omega_R^\dagger)^{Ii} \propto (\hat{Y}_\Delta^d)^{ji} + \mathcal{O}(\eta)$, and it is also vanishing. In the case of $h_\Delta$ and $\Delta_8$ loops, the amplitudes contain the following coupling structure

$$\sum_I (\hat{Y}_\Delta^d)^{jI}(\hat{Y}_\Delta^{d\dagger})^{Ii} \; f'(m_I^d, m_{h_\Delta}), \quad \sum_I (\hat{Y}_\Delta^d)^{jI}(\hat{Y}_\Delta^d)^{Ii} \; g'(m_I^d, m_{h_\Delta}), \qquad (4.21)$$

where $f'$ and $g'$ are different loop functions from $f$ and $g$. Under the conditions (i) and (ii), these are proportional to $\sum_I (\hat{Y}_\Delta^d)^{jI}(\hat{Y}_\Delta^{d\dagger})^{Ii} \simeq \delta^{ji}$ and $\sum_I (\hat{Y}_\Delta^d)^{jI}(\hat{Y}_\Delta^d)^{Ii} \propto (\overline{\Psi}_L)^{ji} \simeq 0$, respectively, and thus the $\overline{d_j} d_i \to \ell\bar{\ell}$ processes do not appear. Moreover, diagrams belonging to the second category allow a lepton flavor violation, such as $\mu \to e$ conversion and $\mu \to e\gamma$, but one can readily show that it is suppressed in a similar manner. We thus conclude that the conditions (i) and (ii) are sufficient to suppress all penguin contributions in the model.

# 5 Summary

In this paper, we study the one-loop contributions to lepton flavor violating decays of neutral mesons composed of down-type quarks in the PS model with vector-like families. These decay modes are known to strongly constrain the scale of the PS symmetry. We clarify the conditions to suppress these decays up to at the one-loop level:

(i) LQ couplings to the SM families are vanishing, i.e. $X_L = X_R \sim 0$.

(ii) Masses of vector-like down-type quarks and charged leptons are individually universal.

(iii) $\Upsilon_L$ and $\Upsilon_R$ have a certain structure such that $K_L \to \mu e$ is sufficiently small.

These are the conditions at the leading order in $\eta := m_{\alpha\beta}/v_\Delta$.

The condition (i) is required to suppress the flavor violations via the tree-level LQ exchange, while the one-loop box diagrams only with the LQ cause the flavor violations only with the condition (i). Note that the tree-level flavor violations via the scalar fields are suppressed independently of the condition (i), as shown in Eqs. (2.32) and (2.33). Once we impose the condition (ii) besides the condition (i), the flavor violating processes from the box diagrams only with the LQ are suppressed due to the unitarity of the LQ gauge couplings, in analogy with the $W$ boson coupling in the SM.

The condition (iii) is necessary to alleviate the constraints from the lepton flavor violating decays induced by the box diagrams involving both vector LQ and scalars. We found that those

diagrams are not suppressed even with the conditions (i) and (ii). Such contribution is well represented by a coupling structure $\Upsilon_A$ ($A = L, R$) defined in Eq. (3.17), whose SM blocks $\Upsilon_A^{ij}$ are the $3 \times 3$ unitary matrices. Because of the unitarity of $\Upsilon_A^{ij}$, we cannot realize $\Upsilon_A^{ij} = 0$ namely no flavor violation. Thus, $\Upsilon_A^{ij}$ should have a structure in such a way that $K_L \to \mu e$ among the flavor violating decays is sufficiently suppressed. This is what the condition (iii) means.

To evaluate the change of the limit depending on the $\Upsilon_A^{ij}$ structure, we studied two simplified cases defined in Eq. (4.19), which correspond to the strongest and weakest limits respectively. In the case (a), the structure of $\Upsilon_A^{ij}$ allows the chiral enhanced $K_L \to \mu e$ decay, and hence $\mathcal{O}(10 \text{ TeV})$ LQ mass is required to be consistent with the experimental limit. It is remarkable that there are upper bounds on the vector-like fermions masses of $\mathcal{O}(\text{TeV})$ to respect $K_L \to \mu e$. This result would encourage direct searches for the vector-like fermions at the LHC and other future collider experiments to test this scenario. In the case (b), $K_L \to \mu e$ is not induced because of the structure of $\Upsilon_A^{ij}$, and hence $B_d \to \tau \mu$ gives the most stringent bound. Since the experimental limits are much weaker for this decay mode, 2 TeV LQ is not excluded by the leptonic decays of the neutral mesons.

In this paper, we suggested the conditions (i)-(iii) to suppress the lepton flavor violating decays of neutral mesons, especially $K_L \to \mu e$. It will be interesting to study what will be caused by violations of these conditions. In particular, the tree-level contributions, namely the violation of the condition (i) is required to explain the $R_{K^{(*)}}$ anomaly, so the full numerical analysis with both tree-level and 1-loop contributions is important. Furthermore, this model could perhaps explain the anomaly in muon $g - 2$ via the loop diagrams involving LQ, vector-like fermions and exotic scalar particles. We leave those extended studies including the violations of three conditions for future work.

# Acknowledgment

# A   Loop functions

The forms of the loop functions are shown in this appendix. Defining

$$F_n(m_1, m_2; M_1, M_2) := \int \frac{d^4 p}{(4\pi)^4} \frac{p^{2n}}{(p^2 - m_1^2)(p^2 - m_2^2)(p^2 - M_1^2)(p^2 - M_2^2)}, \qquad (A.1)$$

those for $n = 0, 1$ are given by

$$F_0(m_1, m_2; M_1, M_2) = \frac{-i}{16\pi^2} \frac{1}{M_1^4} \left\{ F(x_1, x_2, \eta) + F(x_2, x_1, \eta) + F(\eta, x_1, x_2) \right\}, \tag{A.2}$$

$$F_1(m_1, m_2; M_1, M_2) = \frac{-i}{16\pi^2} \frac{1}{M_1^2} \left\{ x_1 F(x_1, x_2, \eta) + x_2 F(x_2, x_1, \eta) + \eta F(\eta, x_1, x_2) \right\}, \tag{A.3}$$

where $x_1 = m_1^2/M_1^2$, $x_2 = m_2^2/M_1^2$, $\eta = M_2^2/M_1^2$. The function $F$ is defined as

$$F(x_1, x_2, \eta) = \frac{x_1 \ln x_1}{(x_1 - 1)(x_1 - x_2)(x_1 - \eta)}. \tag{A.4}$$

If $m := m_1 = m_2$ and $M := M_1 = M_2$, these are simplified to

$$F_0(m, M) = \frac{-i}{16\pi^2 M^4} \frac{2(1 - x) + (1 + x)\log x}{(1 - x)^3}, \tag{A.5}$$

$$F_1(m, M) = \frac{-i}{16\pi^2 M^2} \frac{1 - x^2 + 2x\log x}{(1 - x)^3}, \tag{A.6}$$

where $x := m^2/M^2$. The dimensionless functions $G_n$, $n = 0, 1$, are the linear combinations of $F_0$ and $F_1$, given by

$$m_X^{2n-4} G_n(m_E, m_D; m_X, m_{h_\Delta}) := \frac{3}{8} F_n(m_E, m_E; m_X, m_{h_\Delta}) + \frac{11}{8} F_n(m_D, m_D; m_X, m_{h_\Delta})$$
$$+ \frac{1}{4} F_n(m_E, m_D; m_X, m_{h_\Delta}). \tag{A.7}$$

We also define $\widetilde{F}_0(m_E, m_D; m_X, m_{h_\Delta}) := m_X^4 F_0(m_E, m_D; m_X, m_{h_\Delta})$, where $\widetilde{F}_0$ is a dimensionless function.

# B   Tree-level constraints

When the LQ mass is 5 TeV, tree-level LQ exchange contributes to lepton flavor violating processes. In particular, $e-\mu$ flavor violating phenomena strongly constrain the coupling products involving first two generations (Table 4). The LQ carries a lepton number, and the family number conserving couplings with LQ lead lepton flavor violating processes e.g. $K_L \to \mu e$. $\mu-e$ conversion process also brings a stringent constraint on the coupling products. In order to avoid the the experimental constraints, those couplings need to be smaller than $\mathcal{O}(10^{-2\sim3})$, assuming that all the couplings have a comparable size. Furthermore one-loop induced $\mu \to e\gamma$ can constrain coupling products. It however depends on the LQ couplings to the vector-like quarks [31], so that we do not discuss it further. For the more generic analysis readers are referred to Ref. [41].

The $h_\Delta$ and $\Delta_8$ exchanging also contributes to flavor violating processes. The scalar couplings with the SM fermions are generally flavor violating and linear to

$$\left( \hat{g}_{d_L}^X \right)_{iD} m_D^e \left( \hat{g}_{d_R}^X \right)_{Dj}^\dagger, \quad \left( \hat{g}_{d_L}^X \right)_{iD}^\dagger m_D^d \left( \hat{g}_{d_R}^X \right)_{Dj}. \tag{B.1}$$

Table 4: The upper limit on the coupling products contributing to the $\mu-e$ flavor violating processes.

| coupling product | | upper limit | process | bound |
|---|---|---|---|---|
| $\left\|\left(\hat{g}_{d_L}^X\right)_{de}\left(\hat{g}_{d_R}^X\right)_{s\mu}\right\|$, $\left\|\left(\hat{g}_{d_R}^X\right)_{de}\left(\hat{g}_{d_L}^X\right)_{s\mu}\right\|$ | | $\lesssim 10^{-5}$ | $K_L \to \mu e$ | [36] |
| $\left\|\left(\hat{g}_{d_L}^X\right)_{se}\left(\hat{g}_{d_R}^X\right)_{d\mu}\right\|$, $\left\|\left(\hat{g}_{d_R}^X\right)_{se}\left(\hat{g}_{d_L}^X\right)_{d\mu}\right\|$ | | $\lesssim 10^{-5}$ | $K_L \to \mu e$ | [36] |
| | $\left\|\left(\hat{g}_{d_L}^X\right)_{de}\left(\hat{g}_{d_L}^X\right)_{d\mu}\right\|$ | $\lesssim 10^{-4}$ | $\mu-e$ conversion | [42] |
| | $\left\|\left(\hat{g}_{d_R}^X\right)_{de}\left(\hat{g}_{d_R}^X\right)_{d\mu}\right\|$ | $\lesssim 10^{-5}$ | $\mu-e$ conversion | [42] |
| | $\left\|\left(\hat{g}_{d_L}^X\right)_{de}\left(\hat{g}_{d_R}^X\right)_{d\mu}\right\|$ | $\lesssim 10^{-5}$ | $\mu-e$ conversion | [42] |
| | $\left\|\left(\hat{g}_{d_L}^X\right)_{se}\left(\hat{g}_{d_R}^X\right)_{s\mu}\right\|$ | $\lesssim 10^{-5}$ | $\mu-e$ conversion | [42] |

As we see in the main text, the scalar couplings are related to the LQ couplings involving heavy fermions as well as SM fermions. Taking into account the tree-level exchanging of $h_\Delta$ and $\Delta_8$ and fixing $m_{h_\Delta} = m_{\Delta_8} = 5\,\text{TeV}$, we can also derive the experimental constraints on the scalar couplings

$$\frac{1}{3}\sqrt{\frac{3}{8}}\left(\left|\hat{Y}_{\Delta\,ij}^d\right|\right) \le \begin{pmatrix} 5\times 10^{-3} & 10^{-5} & 10^{-3} \\ 10^{-5} & 1\times 10^{-2} & 5\times 10^{-3} \\ 10^{-3} & 5\times 10^{-3} & 1 \end{pmatrix}, \tag{B.2}$$

$$\sqrt{\frac{3}{8}}\left(\left|\hat{Y}_{\Delta\,ij}^e\right|\right) \le \begin{pmatrix} 1 & 1\times 10^{-3} & 0.5 \\ 1\times 10^{-3} & 1 & 0.5 \\ 0.5 & 0.5 & 1 \end{pmatrix}. \tag{B.3}$$

The upper bounds on off-diagonal elements of $\hat{Y}_{\Delta\,ij}^d$ are given by $K\text{-}\overline{K}$, $B\text{-}\overline{B}$ and $B_s\text{-}\overline{B_s}$ mixings. The bounds on off-diagonal elements of $\hat{Y}_{\Delta\,ij}^e$ are derived from $\mu \to 3e$, $\tau \to \ell\ell\ell'$, by setting all diagonal elements to unity. The bounds on diagonal elements of $\hat{Y}_{\Delta\,ij}^d$ are derived from the $\mu\text{-}e$ conversion with the maximally allowed $\hat{Y}_{\Delta\,e\mu}^e$. As is discussed in the main text, the conditions (i) and (ii) suppress those dangerous couplings.

# References

[1] J. C. Pati and A. Salam, *Lepton Number as the Fourth Color*, *Phys. Rev. D* **10** (1974) 275–289.

[2] LHCᴮ collaboration, R. Aaij et al., *Measurement of Form-Factor-Independent Observables in the Decay $B^0 \to K^{*0}\mu^+\mu^-$*, *Phys. Rev. Lett.* **111** (2013) 191801, [1308.1707].

[3] LHCᴮ collaboration, R. Aaij et al., *Test of lepton universality with $B^0 \to K^{*0}\ell^+\ell^-$ decays*, *JHEP* **08** (2017) 055, [1705.05802].

[4] LHCʙ collaboration, R. Aaij et al., *Test of lepton universality using $B^+ \to K^+\ell^+\ell^-$ decays*, *Phys. Rev. Lett.* **113** (2014) 151601, [1406.6482].

[5] LHCʙ collaboration, R. Aaij et al., *Search for lepton-universality violation in $B^+ \to K^+\ell^+\ell^-$ decays*, *Phys. Rev. Lett.* **122** (2019) 191801, [1903.09252].

[6] LHCʙ collaboration, R. Aaij et al., *Angular analysis of the $B^0 \to K^{*0}\mu^+\mu^-$ decay using 3 $fb^{-1}$ of integrated luminosity*, *JHEP* **02** (2016) 104, [1512.04442].

[7] LHCʙ collaboration, R. Aaij et al., *Measurement of $CP$-Averaged Observables in the $B^0 \to K^{*0}\mu^+\mu^-$ Decay*, *Phys. Rev. Lett.* **125** (2020) 011802, [2003.04831].

[8] LHCʙ collaboration, R. Aaij et al., *Angular Analysis of the $B^+ \to K^{*+}\mu^+\mu^-$ Decay*, *Phys. Rev. Lett.* **126** (2021) 161802, [2012.13241].

[9] LHCʙ collaboration, R. Aaij et al., *Tests of lepton universality using $B^0 \to K_S^0\ell^+\ell^-$ and $B^+ \to K^{*+}\ell^+\ell^-$ decays*, 2110.09501.

[10] G. Isidori, S. Nabeebaccus and R. Zwicky, *QED corrections in $\overline{B} \to \overline{K}\ell^+\ell^-$ at the double-differential level*, *JHEP* **12** (2020) 104, [2009.00929].

[11] BaBar collaboration, J. Lees et al., *Evidence for an excess of $\bar{B} \to D^{(*)}\tau^-\bar{\nu}_\tau$ decays*, *Phys. Rev. Lett.* **109** (2012) 101802, [1205.5442].

[12] BaBar collaboration, J. Lees et al., *Measurement of an Excess of $\bar{B} \to D^{(*)}\tau^-\bar{\nu}_\tau$ Decays and Implications for Charged Higgs Bosons*, *Phys. Rev. D* **88** (2013) 072012, [1303.0571].

[13] Belle collaboration, M. Huschle et al., *Measurement of the branching ratio of $\bar{B} \to D^{(*)}\tau^-\bar{\nu}_\tau$ relative to $\bar{B} \to D^{(*)}\ell^-\bar{\nu}_\ell$ decays with hadronic tagging at Belle*, *Phys. Rev. D* **92** (2015) 072014, [1507.03233].

[14] Belle collaboration, Y. Sato et al., *Measurement of the branching ratio of $\bar{B}^0 \to D^{*+}\tau^-\bar{\nu}_\tau$ relative to $\bar{B}^0 \to D^{*+}\ell^-\bar{\nu}_\ell$ decays with a semileptonic tagging method*, *Phys. Rev. D* **94** (2016) 072007, [1607.07923].

[15] Belle collaboration, S. Hirose et al., *Measurement of the $\tau$ lepton polarization and $R(D^*)$ in the decay $\bar{B} \to D^*\tau^-\bar{\nu}_\tau$*, *Phys. Rev. Lett.* **118** (2017) 211801, [1612.00529].

[16] Belle collaboration, A. Abdesselam et al., *Measurement of $\mathcal{R}(D)$ and $\mathcal{R}(D^*)$ with a semileptonic tagging method*, 1904.08794.

[17] LHCʙ collaboration, R. Aaij et al., *Measurement of the ratio of branching fractions $\mathcal{B}(\bar{B}^0 \to D^{*+}\tau^-\bar{\nu}_\tau)/\mathcal{B}(\bar{B}^0 \to D^{*+}\mu^-\bar{\nu}_\mu)$*, *Phys. Rev. Lett.* **115** (2015) 111803, [1506.08614].

[18] LHCʙ collaboration, R. Aaij et al., *Test of Lepton Flavor Universality by the measurement of the $B^0 \to D^{*-}\tau^+\nu_\tau$ branching fraction using three-prong $\tau$ decays*, *Phys. Rev. D* **97** (2018) 072013, [1711.02505].

[19] S. Iguro and R. Watanabe, *Bayesian fit analysis to full distribution data of* $\overline{\mathrm{B}} \to \mathrm{D}^{(*)}\ell\overline{\nu} : |\mathrm{V}_{\mathrm{cb}}|$ *determination and new physics constraints*, *JHEP* **08** (2020) 006, [2004.10208].

[20] Y. Aoki et al., *FLAG Review 2021*, 2111.09849.

[21] Muon g-2 collaboration, G. W. Bennett et al., *Final Report of the Muon E821 Anomalous Magnetic Moment Measurement at BNL*, *Phys. Rev. D* **73** (2006) 072003, [hep-ex/0602035].

[22] Muon g-2 collaboration, B. Abi et al., *Measurement of the Positive Muon Anomalous Magnetic Moment to 0.46 ppm*, *Phys. Rev. Lett.* **126** (2021) 141801, [2104.03281].

[23] T. Aoyama et al., *The anomalous magnetic moment of the muon in the Standard Model*, *Phys. Rept.* **887** (2020) 1–166, [2006.04822].

[24] F. S. Queiroz and W. Shepherd, *New Physics Contributions to the Muon Anomalous Magnetic Moment: A Numerical Code*, *Phys. Rev. D* **89** (2014) 095024, [1403.2309].

[25] C. Biggio, M. Bordone, L. Di Luzio and G. Ridolfi, *Massive vectors and loop observables: the $g − 2$ case*, *JHEP* **10** (2016) 002, [1607.07621].

[26] S. M. Bilenky and S. T. Petcov, *Massive Neutrinos and Neutrino Oscillations*, *Rev. Mod. Phys.* **59** (1987) 671.

[27] P. Hung, A. Buras and J. Bjorken, *Petite Unification of Quarks and Leptons*, *Phys. Rev. D* **25** (1982) 805.

[28] G. Valencia and S. Willenbrock, *Quark - lepton unification and rare meson decays*, *Phys. Rev. D* **50** (1994) 6843–6848, [hep-ph/9409201].

[29] L. Calibbi, A. Crivellin and T. Li, *Model of vector leptoquarks in view of the B-physics anomalies*, *Phys. Rev. D* **98** (2018) 115002, [1709.00692].

[30] M. J. Dolan, T. P. Dutka and R. R. Volkas, *Lowering the scale of Pati-Salam breaking through seesaw mixing*, *JHEP* **05** (2021) 199, [2012.05976].

[31] S. Iguro, J. Kawamura, S. Okawa and Y. Omura, *TeV-scale vector leptoquark from Pati-Salam unification with vectorlike families*, *Phys. Rev. D* **104** (2021) 075008, [2103.11889].

[32] L. Di Luzio, J. Fuentes-Martin, A. Greljo, M. Nardecchia and S. Renner, *Maximal Flavour Violation: a Cabibbo mechanism for leptoquarks*, *JHEP* **11** (2018) 081, [1808.00942].

[33] J. Fuentes-Martín, G. Isidori, M. König and N. Selimović, *Vector Leptoquarks Beyond Tree Level III: Vector-like Fermions and Flavor-Changing Transitions*, *Phys. Rev. D* **102** (2020) 115015, [2009.11296].

[34] D. Marzocca, *Addressing the B-physics anomalies in a fundamental Composite Higgs Model*, *JHEP* **07** (2018) 121, [1803.10972].

[35] S. L. Glashow, J. Iliopoulos and L. Maiani, *Weak Interactions with Lepton-Hadron Symmetry*, *Phys. Rev. D* **2** (1970) 1285–1292.

[36] PARTICLE DATA GROUP collaboration, P. Zyla et al., *Review of Particle Physics*, *PTEP* **2020** (2020) 083C01.

[37] FLAVOUR LATTICE AVERAGING GROUP collaboration, S. Aoki et al., *FLAG Review 2019: Flavour Lattice Averaging Group (FLAG)*, *Eur. Phys. J. C* **80** (2020) 113, [1902.08191].

[38] ATLAS collaboration, M. Aaboud et al., *Search for large missing transverse momentum in association with one top-quark in proton-proton collisions at $\sqrt{s}$ = 13 TeV with the ATLAS detector*, *JHEP* **05** (2019) 041, [1812.09743].

[39] CMS collaboration, A. M. Sirunyan et al., *Search for electroweak production of a vector-like T quark using fully hadronic final states*, *JHEP* **01** (2020) 036, [1909.04721].

[40] ATLAS collaboration, G. Aad et al., *Search for high-mass dilepton resonances using 139 fb$^{-1}$ of pp collision data collected at $\sqrt{s}$ =13 TeV with the ATLAS detector*, *Phys. Lett. B* **796** (2019) 68–87, [1903.06248].

[41] B. Fornal, S. A. Gadam and B. Grinstein, *Left-Right SU(4) Vector Leptoquark Model for Flavor Anomalies*, *Phys. Rev. D* **99** (2019) 055025, [1812.01603].

[42] SINDRUM II collaboration, W. H. Bertl et al., *A Search for muon to electron conversion in muonic gold*, *Eur. Phys. J. C* **47** (2006) 337–346.